Int J Clin Exp Med 2017;10(7):10049-10057
www.ijcem.com /ISSN:1940-5901/IJCEM0050615

Original Article

Construction of porous bFGF-PLGA-HAP-PLLA microsphere and its biocompatibility with bone marrow mesenchymal stem cells

Yong Zheng[1,2], Junying Sun[1]

[1]*Department of Orthopaedics, The First Affiliated Hospital of Soochow University, Suzhou, Jiangsu, China;* [2]*Department of Orthopaedics, Jiangbei People's Hospital, Nanjing, Jiangsu, China*

Received February 11, 2017; Accepted March 7, 2017; Epub July 15, 2017; Published July 30, 2017

Abstract: Background: The innovative repair materials for the bones are still lacking. So, we synthesized a porous microsphere by using basic fibroblast growth factor (bFGF), polylactide-co-glycolide (PLGA), poly L-lactic acid (PLLA) and hydroxylapatite (HAP), and its biocompatibility with bone marrow mesenchymal stem cells (BM-MSCs) was investigated in vitro. Methods: A modified solvent extraction/evaporation double emulsion method was used to first prepare PLGA and bFGF-PLGA microspheres. The morphologies and surface characteristics of PLGA microspheres and bFGF-PLGA microspheres were observed by using laser diffraction particle size analyzer and transmission electron microscopy (TEM). Drug release patterns of bFGF-PLGA microspheres in vitro were also examined. The porous bFGF-PLGA-HAP-PLLA microspheres were then fabricated with PLLA, HAP and the bFGF-PLGA microspheres and subjected to thermal analysis, scanning electron microscope (SEM) for surface morphology detection and X-ray diffraction (XRD) analysis and fourier transform infrared spectroscopy (FT-IR) spectra analysis. The cytotoxicity and biocompatibility with BM-MSCs in vitro were also tested by measuring BMSCs viability and proliferation by using MTT assay or observed by microscope. Results: The results showed that the particle size of bFGF-PLGA microspheres was about 250 nm with a morphology of mono-disperse spherical without aggregation. The drug release profile of bFGF-PLGA microspheres exhibited the one phase release profile with an initial burst rate of 33% in the first 10 hours, then 70.5% accumulative release after 7 days. Thermal analysis suggested porous materials were decomposed between 250°C~400°C, and the mass of porous materials was reduced extremely in the range of 300°C~350°C and slowly after 400°C because of PLLA, PLGA and HAP property. SEM scanning showed that the appearance of PLGA microspheres was spherical, and the hydroxyapatite was reunited. Synthesized XRD patterns showed that strong Bragg reflections (18.5° and 32°) were seen which correspond to the PLLA and HAP. FT-IR spectra found that the PLLA+HAP+bFGF-PLGA porous material had very similar curve lines to other microspheres. MTT assay and microscopy results suggested the cytotoxicity of bFGF-PLGA+HAP+PLLA porous material met the requirements of the scaffold material in bone tissue engineering and was conducive to promote the proliferation of BM-MSCs. Conclusion: The bFGF-PLGA+HAP+PLLA porous material is successfully prepared and has good biocompatibility with BMSC.

Keywords: Biocompatibility, bone marrow mesenchymal stromal cells, poly, hydroxylapatite, bFGF-PLGA+HAP+PLLA porous material

Introduction

Absorbable synthetic material applying to repair material of bone defects is one of central issues in Orthopedics [1]. Because of its favorable biocompatibility and absorbability, poly L-lactic acid (PLLA) tends to be used more frequently than the others. Hydroxylapatite (HAP), with favorable biocompatibility and bone conduction, can form direct combination with bone structure [2]. Basic fibroblast growth factor (bFGF) plays an important role in morphologic and bone healing processes and is a potent stimulator of osteopathic proliferation. Poly lactic-co-glycolic acid (PLGA), which is a biodegradable material owing to its good biocompatibility, has been used as a carrier of microspheres to parcel drugs and to lengthen the sustained release time. As such, PLGA has been widely used in the pharmaceutical industry [3, 4]. In

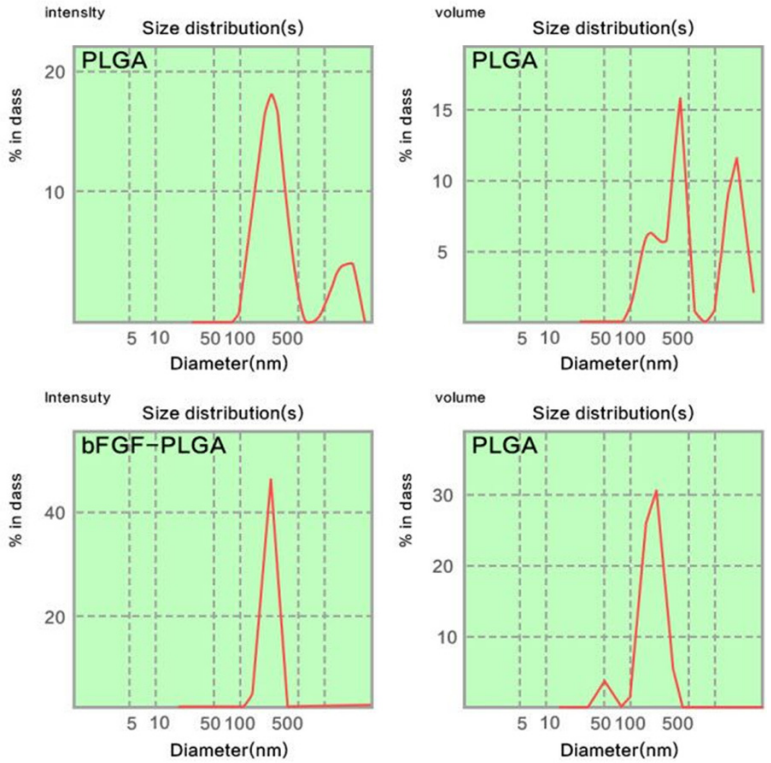

Figure 1. The particle size distribution of microspheres.

earlier studies, the bFGF-PLGA microsphere drug delivery system has been demonstrated to contribute to successful osteoinduction in fractures in animal models [5, 6].

So we chose PLLA as the matrix of the materials, HAP and bFGF-PLGA as the bioactive composition. Additionally, fabricated bFGF-PLGA+PLLA+HAP porous material, and its biocompatibility with bone marrow mesenchymal stromal cells (BM-MSCs) in vitro was investigated.

Materials and methods

Materials

Dichloromethane (AR) and 1, 4-Dioxane were obtained from Kelong Chemical (Chengdu, China). Poly (vinyl alcohol), bFGF and PLGA (molar ratio of *D*, L-lactic to glycolic acid, 50:50) were purchased from Sigma Chemical (St Louis, MO, USA). Poly (L-lactic acid) was supplied by Daigang Biomaterial (Jinan, China). Hydroxyapatite were purchased from Realin Biotechnology (Xi'an, China).

Preparation of BM-MSCs

All procedures concerning animals were approved by the Animal Care and Experiment Committee. BMSCs were isolated and cultured from rats. Briefly, 12-week-old male SD rats with an average weight of 200g ± 12 g were obtained from the Animal Center of People's Liberation Army General Hospital (Beijing, China). After anesthesia, both ends of the femora were cut off at the epiphysis and bone marrow was flushed out with DMEM (Sigma, USA) containing of 10% FBS (Sigma, USA) and 200 units/ml of heparin (Hyclone, USA). Cells were then cultured in DMEM containing 10% FBS, 100 units/ml penicillin, and 100 units/ml streptomycin, supplemented with 50 μg/ml ascorbic acid, 10 mM β-glycerol phosphate, and 10^{-8} M dexamethasone at 37°C under 95% humidity with 5% CO_2. The medium was changed after 4 days and then every 3-4 days until cell confluence. Cells at passage 2-4 were used for the following experiments.

Methods

Preparation of PLGA and bFGF-PLGA microspheres: PLGA microspheres and bFGF-PLGA microspheres were prepared by a modified solvent extraction/evaporation double emulsion method. In brief, 15.0 mg of PVA (200 μL bFGF) was dissolved in 20.0 mL of deionized water as the aqueous phase, which was distributed into the internal aqueous phase and external aqueous phase with certain proportion. Organic phase was prepared by dissolving 40.0 mg of PLGA in 10.0 mL of dichloromethane solution. Then the internal aqueous solution was slowly dropwise, which was taken into organic phase to form stabilized original emulsion under sonication (Ningbo Xinyi ultrasonic equipment Co., Ltd., JY92-IIN) for 120 s at 100 W output. After that, the formed original emulsion was poured into the external aqueous phase, which was sonicated for 180 s at 200 W output. The double emulsion was stirred by vacuum rotary evaporation (Shanghai Jukun Vacuum Instrument Equipment Co., Ltd., R210D) to allow the organic solvent to completely evaporate.

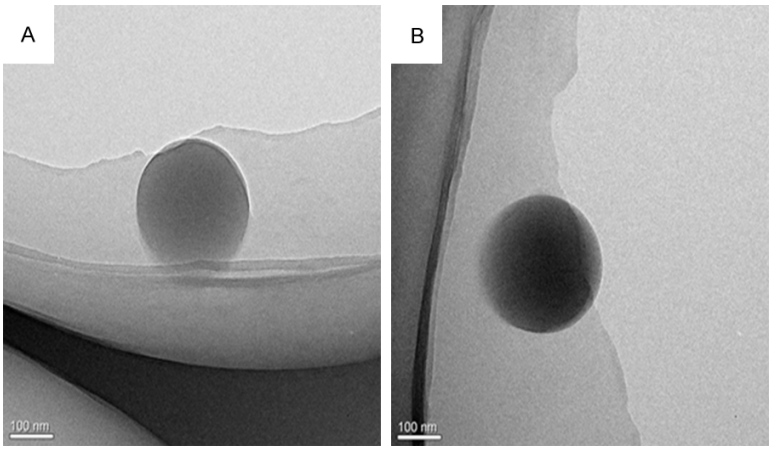

Figure 2. TEM imaging of microspheres: A. (PLGA); B. (bFGF-PLGA).

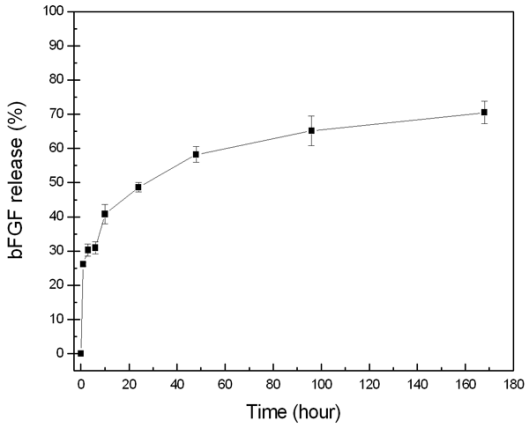

Figure 3. The release of bFGF from bFGF-PLGA microspheres.

PLGA and bFGF-PLGA microspheres size determination: About 0.2 mL of PLGA microspheres and bFGF-PLGA microspheres suspensions were diluted into 2.5 mL of water immediately after preparation respectively. The average particle size was determined by quasielastic laser light scattering with a Malvern Zetasizer (Malvern Instruments Limited, Mastersizer 2000) at 25°C.

Transmission electron microscopy imaging of PLGA and bFGF-PLGA microspheres: The morphologies of PLGA microspheres and bFGF-PLGA microspheres were observed by using transmission electron microscopy (TEM). (JEOL, Ltd., JEOL-100C XII). The PLGA microspheres and bFGF-PLGA microspheres solutions wanted to be determined were placed on a copper grid coated with film.

Drug release test of bFGF-PLGA microspheres in vitro: The release profiles of bFGF from bFGF-PLGA microspheres in vitro were determined as follows: 1.0 mL (1.0 mg/mL) of bFGF-PLGA microspheres solution was added to a dialysis bag with 20.0 mL of phosphate buffer solution (PBS) (0.1 M, pH 7.4) in test tubes and incubated at 37 ± 0.5°C with shaking at 100 rpm. At the designated time intervals, buffer solution within the dialysis bag was removed for testing. The amount of bFGF released from bFGF-PLGA microspheres was quantified with UV-Vis spectroscopy (Shanghai Precision & Scientific Instrument Co., Ltd., 752N).

Preparation of porous bFGF-PLGA-HAP-PLLA materials: PLLA was dissolved in 5 mL of 1, 4-Dioxane, and bFGF, HAP, PLGA or bFGF-PLGA was added into this solution. Then the solution was heated with frequent agitation to completely dissolve the powder. The emulsion was cooled to -20°C in a refrigerator and the solid emulsion was lyophilized overnight. The PLLA+HAP+bFGF-PLGA porous material was obtained after dissolving NaCl by water.

FT-IR measurement of porous materials: FT-IR spectra (Fourier transform infrared spectra) of porous materials was recorded with KBr pellets (Bruker Corporation, TENSOR27) within the scan range of 400~4000 cm^{-1}. The samples were thoroughly milled with KBr and pressed into pellets.

Thermo gravimetric analysis of porous materials: The thermo gravimetric analysis of porous materials in the temperature range between 30 and 600°C was performed by using a simultaneous thermal analyzing system (STA 409/CMS, Netzsch; heating rate, 20°C/min) in combination with a mass spectroscopic detection unit (QMG 421, Balzer).

X-ray diffraction (XRD) measurements of porous materials: XRD analysis of the prepared porous materials was performed by using an X' Pert PRO of PANalytical diffract meter. The Cu-Kα X-rays of wavelength (λ) was 1.54056 Å

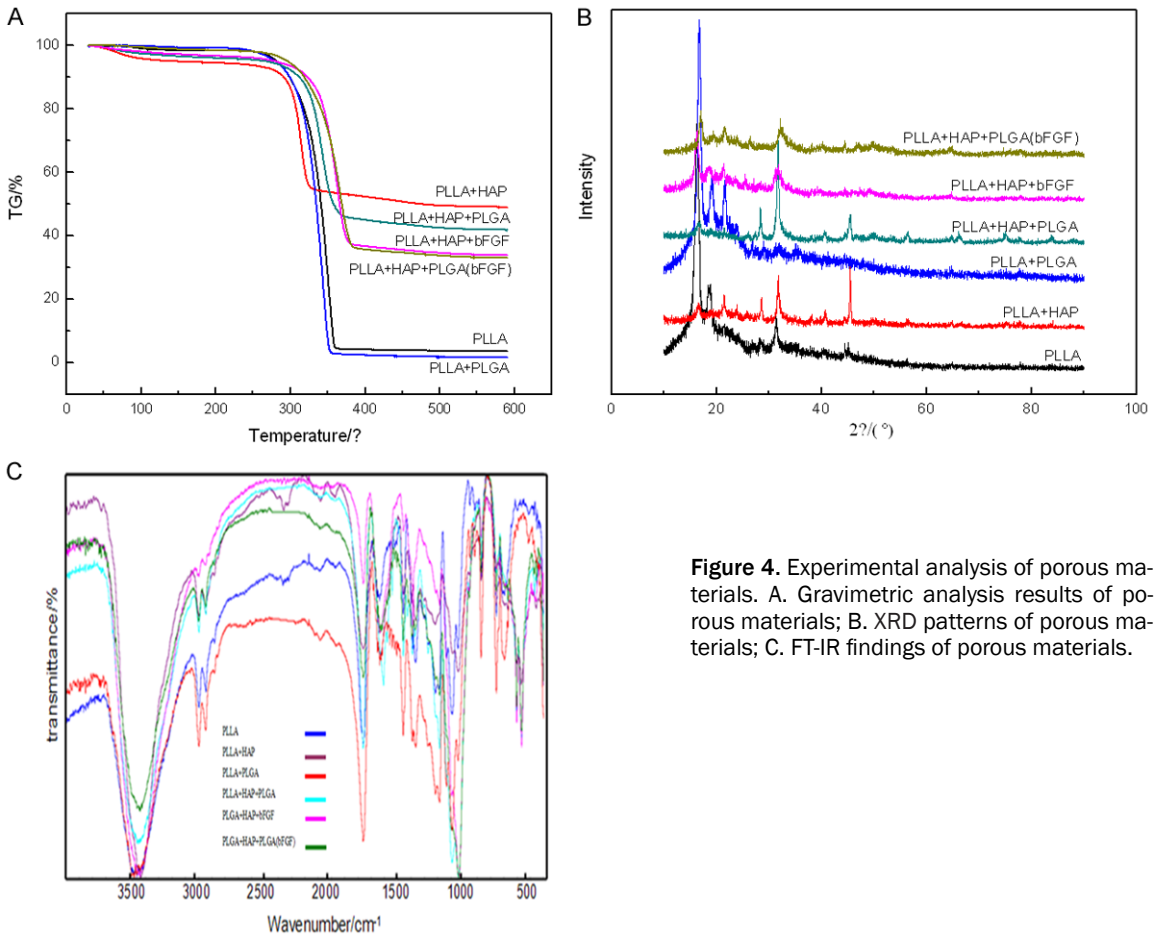

Figure 4. Experimental analysis of porous materials. A. Gravimetric analysis results of porous materials; B. XRD patterns of porous materials; C. FT-IR findings of porous materials.

and data was taken for the 2θ range of 10° to 90° with a step of 0.02°.

Scanning electron microscopy imaging of porous materials: Scanning electron microscopy (SEM) imaging of cylindrical porous materials was obtained by a Hitachi S-4800 field-emission SEM.

Evaluation of cytotoxicity of porous materials using the MTT assay: The MTT assay was used to assess the cytotoxicity of porous materials in vitro. Rat BM-MSCs (100 μl; $1*10^5$ cells/mL) were seeded into 96 well microplates and cultured according to manufacturer instructions. Then BM-MSCs were co-cultured with porous materials for 48 h. Thereafter, the relative optical density was measured wtih Well scan Mk3 microplate reader (Labsystems Dragon) at wavelength of 570 nm. The relative cell viability of each parallel experimental group was expressed as percentage (%) of that without treatment (control).

Evaluation of BM-MSCs growth using flow cytometry: Growth curves were determined to ensure that cells used in experiments were within the exponential growth phase. Cell proliferation was assessed by flow cytometry and fluorescence microscope. Rat BM-MSCs (100 μl/well) were seeded at seeding densities of $1*10^5$ cells/mL into 96 well microtitre plates, and porous materials ($6.0*10^5$/ml) were applied to the cells for 48 h. The viability of rat BM-MSCs was assessed after the porous materials were removed and BM-MSCs were labeled by FITC.

Statistical analysis

Statistical analysis was performed by using SPSS 19.0 software (IBM, USA). Data were expressed as mean ± standard deviation (SD). One-way ANOVA with post hoc Bonferroni test was used to analyze intergroup differences on cell viability and cell growth. $P<0.05$ (two-sided) was considered statistically significant.

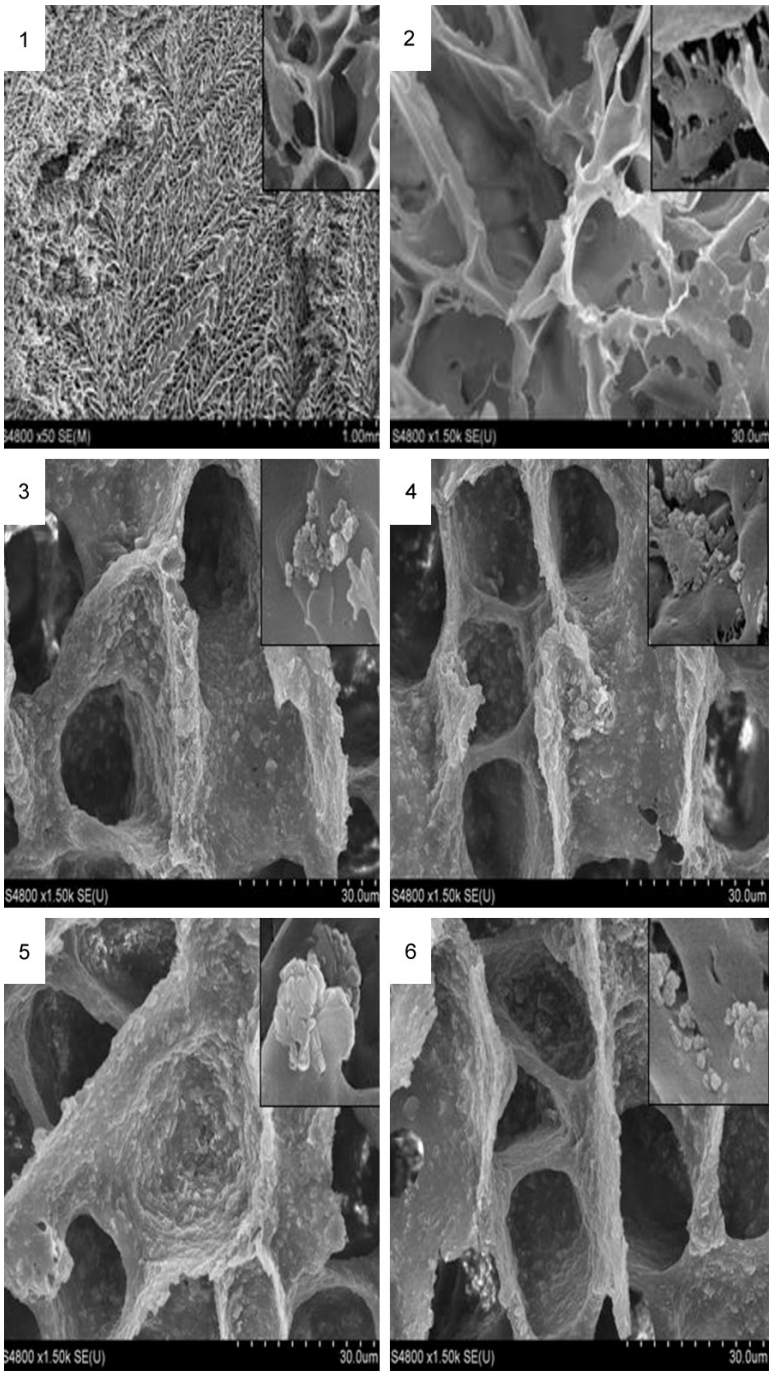

Figure 5. Scanning electron microscope of porous materials Scanning electron microscope of PLLA (1), PLLA+PLGA (2), PLLA+HAP (3), PLLA+HAP+PLGA (4), PLLA+HAP+bFGF (5), PLLA+HAP+bFGF-PLGA (6).

Results

Particle size of PLGA and bFGF-PLGA microspheres

Size distribution of PLGA microspheres and bFGF-PLGA microspheres are shown in **Figure 1**. The average particle size (hydrodynamic diameter) of PLGA microspheres was 254.9 nm with a polydispersity index of 0.29. The average particle size (hydrodynamic diameter) of bFGF-PLGA microspheres was 231.0 with a polydispersity index of 0.26.

Surface morphology of PLGA and bFGF-PLGA microspheres

TEM imaging of revealed that PLGA microspheres and bFGF-PLGA microspheres were both ~200 nm spheres with smooth surfaces (**Figure 2**).

bFGF release from bFGF-PLGA microspheres

The drug release profile of bFGF-PLGA microspheres is presented in **Figure 3**, which exhibits the one phase release profile with an initial burst rate of 33% in the first 10 hours. After 7 days, 70.5% accumulative release of bFGF was found.

Thermal analysis, XRD and FT-IR measurement of porous materials

As shown in **Figure 4A**, with the thermal analysis performed under air, porous materials were decomposed between 250°C~400°C. The mass of porous materials were extremely reduced in the range of 300°C~350°C, and the mass of porous materials was reduced slowly after 400°C. The XRD patterns of the porous materials synthesized are shown in **Figure 4B**. Strong Bragg reflections (18.5° and 32°) were seen which correspond to the PLLA and HAP. Fourier transform infrared spectroscopy (FT-IR) spectra found that the PLLA+HAP+bFGF-PLGA porous material had very similar curve lines to PLLA, PLLA+HAP, PLLA+PLGA, PLLA+HAP+PLGA and PLLA+HAP+bFGF microspheres (**Fig-**

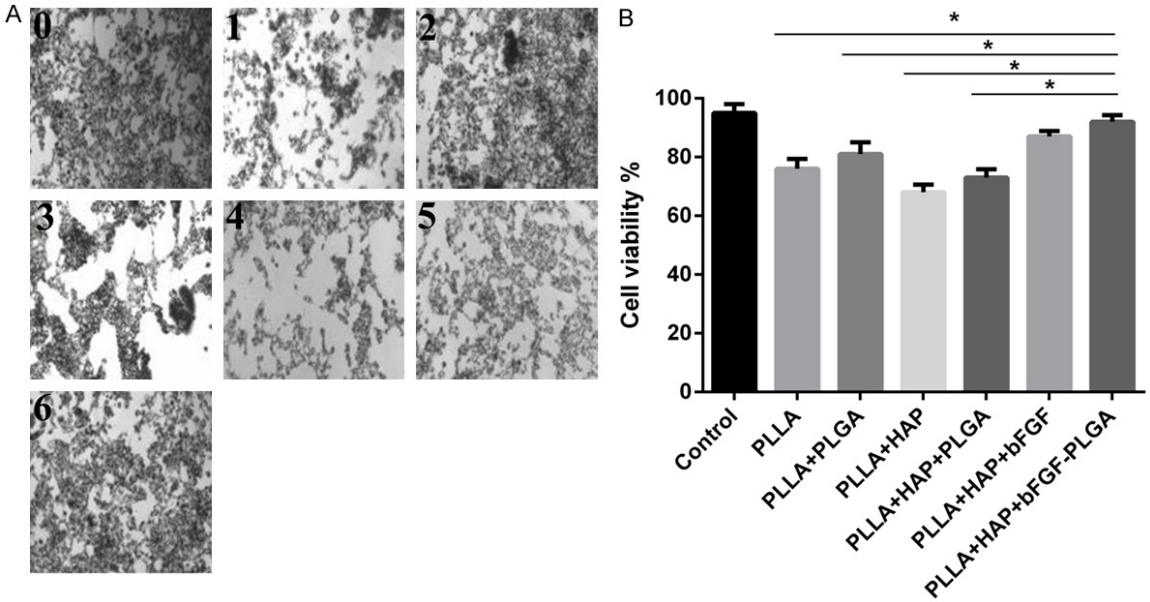

Figure 6. Evaluation of the cytotoxicity of porous materials. A. The number of BM-MSCs co-cultured with control (0), PLLA (1), PLLA+PLGA (2), PLLA+HAP (3), PLLA+HAP+PLGA (4), PLLA+HAP+bFGF (5), PLLA+HAP+bFGF-PLGA (6) observed by microscope; B. MTT assay for viability estimation of BM-MSCs co-cultured with control, PLLA, PLLA+PLGA, PLLA+HAP, PLLA+HAP+PLGA, PLLA+HAP+bFGF, PLLA+HAP+bFGF-PLGA, *P<0.05.

ure 4C). The main peaks were attributed to PLLA, PLGA and HAP.

Scanning electron microscope of porous materials

The results of surface morphological by using SEM were represented in **Figure 5**. The results showed that the porous materials had uniform pore size distribution; PLGA microspheres were obtained and the appearance was spherical. And the result showed that PLGA microspheres and hydroxyapatite were obtained. The appearance of PLGA microspheres was spherical, and the hydroxyapatite was reunited.

Cytotoxicity of porous materials

According to the **Figure 6A**, there were a greater number of BM-MSCs than other groups observed by microscope, which suggested the cytotoxicity of PLLA+HAP+bFGF-PLGA porous material was minimal. The results of the relative cell viability showed the number of BM-MSCs co-cultured with PLLA+HAP+bFGF-PLGA colony per unit volume was significantly higher than those co-cultured with PLLA ($P<0.05$), PLLA+PLGA ($P<0.05$), PLLA+HAP ($P<0.05$), PLLA+HAP+PLGA ($P<0.05$), and there was no difference between the number of BM-MSCs co-cultured with PLLA+HAP+bFGF-PLGA and control (**Figure 6B**).

Effects of porous materials on rat BM-MSCs proliferation

According to **Figure 7A**, PLLA+HAP+bFGF-PLGA porous material was the best beneficial to the proliferation rat of BM-MSCs cells by using flow cytometry. As shown in **Figure 7B**, under the fluorescence microscope, FITC green fluorescence was obviously observed. The number of BM-MSCs was different in the same microscopic field, and the number of rat BM-MSCs cells was the most after joining the PLLA+HAP+bFGF-PLGA porous material.

Discussion

There are tens of millions of bone defect patients caused by accidents or diseases to need rehabilitation therapy every year in China, but the treatment of bone defect has been an unsolved clinical difficult problem [7-9].

In this study, the particle sizes of PLGA microspheres and bFGF-PLGA microspheres were about 250 nm, and the morphology was monodisperse spherical without aggregation; the "burst release behavior" in sustained release

A

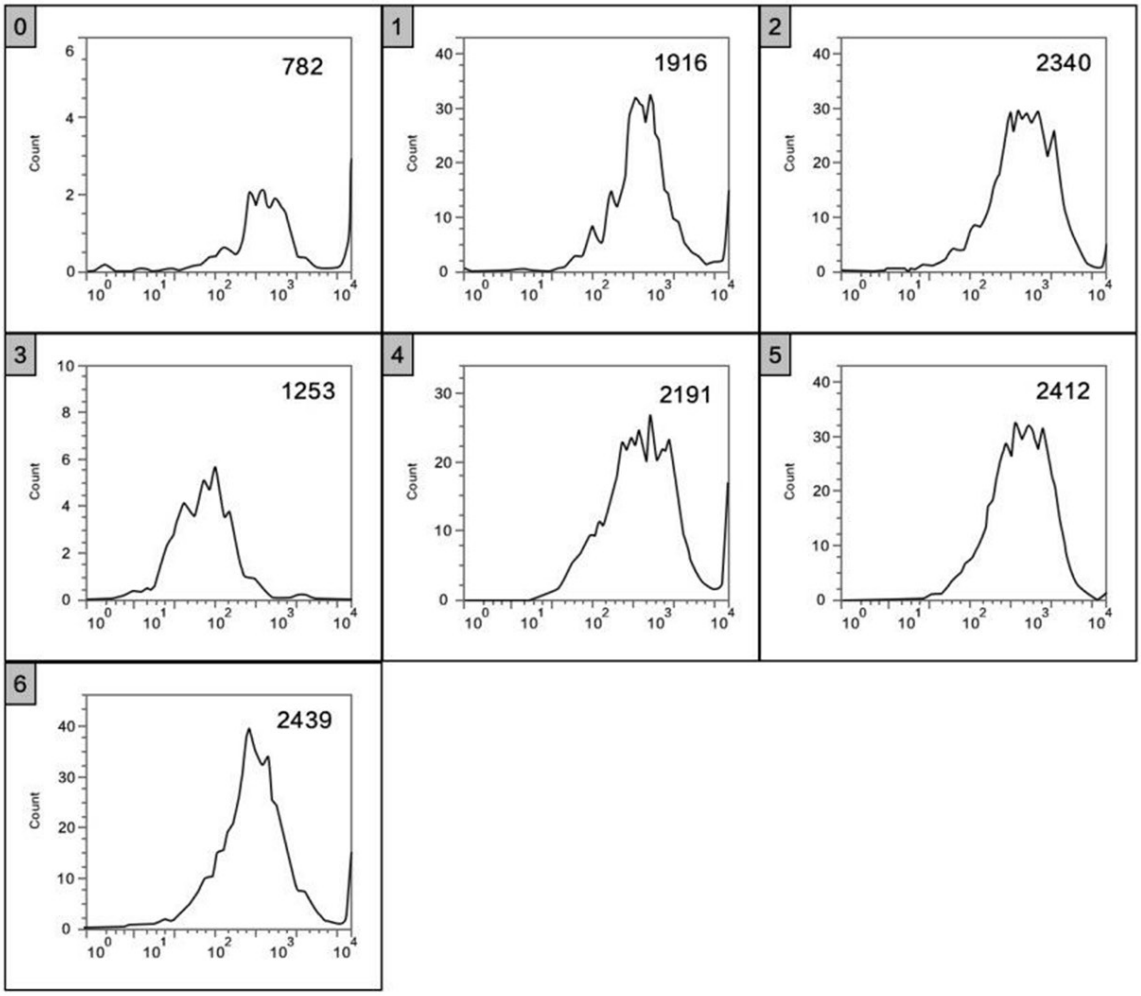

B

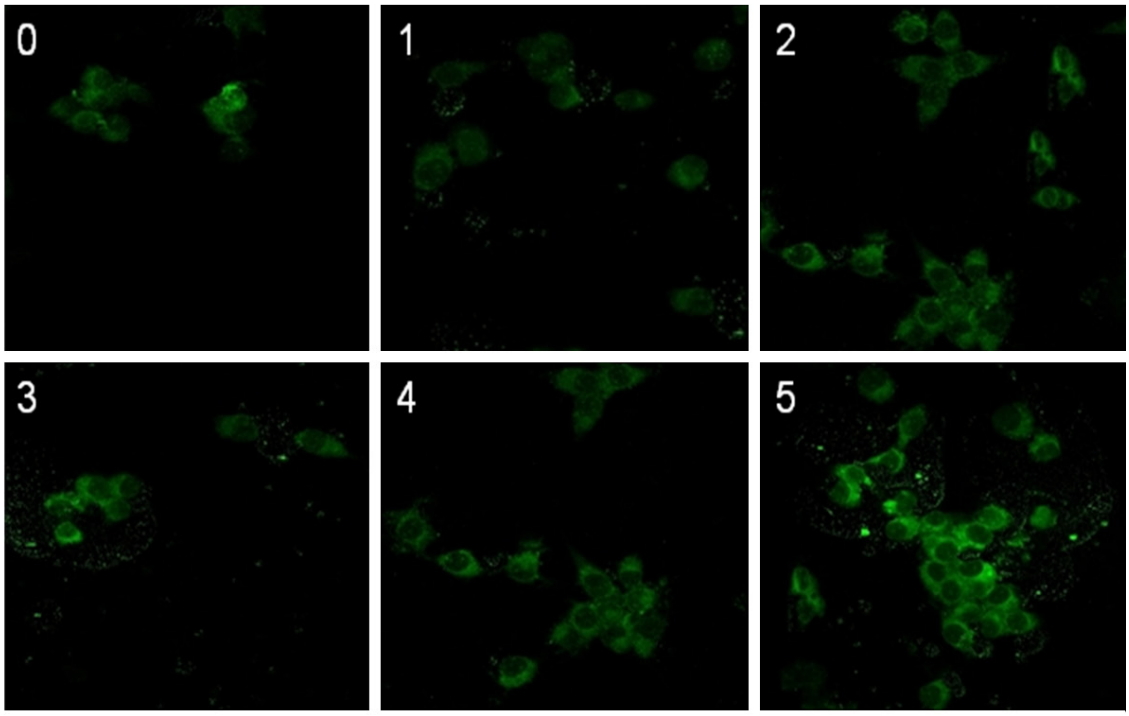

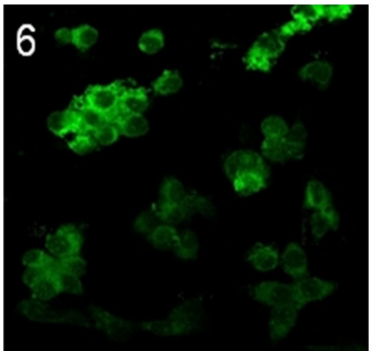

Figure 7. Evaluation of BM-MSCs growth with porous materials. Growth evaluation of BM-MSCs co-cultured with control (0), PLLA (1), PLLA+HAP (2), PLLA+PLGA (3), PLLA+HAP+PLGA (4), PLLA+HAP+bFGF (5), PLLA+HAP+bFGF-PLGA (6), by using flow cytometry (A) and fluorescence microscope (B).

curve of bFGF-PLGA microsphere before 10 h was attributed to fast release of bFGF on the microspheres. However, the characteristic absorption peak of bFGF was not seen in the infrared spectra of porous materials [8, 10, 11], this might because the adding amount of bFGF was few, and bFGF was enwrapped by PLGA microspheres; PLLA and PLGA were decomposed between 250~360°C, and HAP was not decomposed between 0~600°C with the thermal analysis performed under air; the XRD spectra of porous materials mainly showed the absorption peak of PLLA. This was because the crystal size of HAP was small, the diffraction peak was less, and covered by the characteristic peaks of PLLA [12-14]. PLGA and bFGF were amorphous substance, so there were no characteristic peaks in XRD spectrum; according to the results of surface morphological by using SEM, the materials prepared were porous materials, as well as microspheres and hydroxyapatite were obtained in the materials [15].

The bFGF-PLGA+HAP+PLLA porous material was made successfully, because HAP+PLLA was the skeleton material with good uniformity [16]; the porous material was conducive to cellular migration, bone-formation and other physiological activities [17, 18]; the PLGA microspheres loaded with bFGF could exert sustained action, and avoid rapid degradation caused by "burst release" of bFGF [19].

Recent study suggested that current limitations in regenerative strategies included impaired cellular proliferation and differentiation [20]. However, according to our results, PLLA+HAP+bFGF-PLGA porous material with the smallest cytotoxicity was the most conducive to promote the cellular proliferation, which met the requirements of the scaffold material in bone tissue engineering [21]. This porous material was conducive to promote the proliferation of BM-MSCs, which might be because of exerting function of bFGF which could enhance the proliferation and differentiation capabilities of BM-MSCs [22]. And these results above demonstrated the bFGF-PLGA+HAP+PLLA porous material prepared in this experiment had good biocompatibility, which could be the basis for biomaterial and stem cell interactions [23].

In conclusion, our study successfully prepares bFGF-PLGA+HAP+PLLA microspheres, and demonstrates its good biocompatibility with BM-MSCs.

Acknowledgements

We are grateful to Jiefeng Gao of Shanghai Shengna Industrial Co., Ltd. for direct and indirect help to design and finish the partical experiment.

Disclosure of conflict of interest

None.

Address correspondence to: Junying Sun, Department of Orthopaedics, The First Affiliated Hospital of Soochow University, No. 188 Shizi Road, Suzhou 215006, Jiangsu, China. Tel: +86-0512-65223637; Fax: +86-0512-65223637; E-mail: sunjunyingfahsc@sina.com

References

[1] Ranly DM, Lohmann CH, Andreacchio D, Boyan BD and Schwartz Z. Platelet-rich plasma inhibits demineralized bone matrix-induced bone formation in nude mice. J Bone Joint Surg Am 2007; 89: 139-147.

[2] McLaren A. A scientist's view of the ethics of human embryonic stem cell research. Cell Stem Cell 2007; 1: 23-26.

[3] Ogawa T, Kitagawa M and Hirokawa K. Age-related changes of human bone marrow: a histometric estimation of proliferative cells, apoptotic cells, T cells, B cells and macrophages. Mech Ageing Dev 2000; 117: 57-68.
[4] Luth ES, Jun SJ, Wessen MK, Liadaki K, Gussoni E and Kunkel LM. Bone marrow side population cells are enriched for progenitors capable of myogenic differentiation. J Cell Sci 2008; 121: 1426-1434.
[5] Feng W, McCabe NP, Mahabeleshwar GH, Somanath PR, Phillips DR and Byzova TV. The angiogenic response is dictated by beta3 integrin on bone marrow-derived cells. J Cell Biol 2008; 183: 1145-1157.
[6] Scintu F, Reali C, Pillai R, Badiali M, Sanna MA, Argiolu F, Ristaldi MS and Sogos V. Differentiation of human bone marrow stem cells into cells with a neural phenotype: diverse effects of two specific treatments. BMC Neurosci 2006; 7: 14.
[7] Sun X, Gan Y, Tang T, Zhang X and Dai K. In vitro proliferation and differentiation of human mesenchymal stem cells cultured in autologous plasma derived from bone marrow. Tissue Eng Part A 2008; 14: 391-400.
[8] Koon HW, Zhao D, Zhan Y, Moyer MP and Pothoulakis C. Substance P mediates antiapoptotic responses in human colonocytes by Akt activation. Proc Natl Acad Sci U S A 2007; 104: 2013-2018.
[9] Kang MH, Kim DY, Yi JY and Son Y. Substance P accelerates intestinal tissue regeneration after gamma-irradiation-induced damage. Wound Repair Regen 2009; 17: 216-223.
[10] Azuma H, Kido J, Ikedo D, Kataoka M and Nagata T. Substance P enhances the inhibition of osteoblastic cell differentiation induced by lipopolysaccharide from Porphyromonas gingivalis. J Periodontol 2004; 75: 974-981.
[11] An YS, Lee E, Kang MH, Hong HS, Kim MR, Jang WS, Son Y and Yi JY. Substance P stimulates the recovery of bone marrow after the irradiation. J Cell Physiol 2011; 226: 1204-1213.
[12] Lee FY, Choi YW, Behrens FF, DeFouw DO and Einhorn TA. Programmed removal of chondrocytes during endochondral fracture healing. J Orthop Res 1998; 16: 144-150.
[13] Bjurholm A, Kreicbergs A, Brodin E and Schultzberg M. Substance P- and CGRP-immunoreactive nerves in bone. Peptides 1988; 9: 165-171.
[14] Mrak E, Guidobono F, Moro G, Fraschini G, Rubinacci A and Villa I. Calcitonin gene-related peptide (CGRP) inhibits apoptosis in human osteoblasts by beta-catenin stabilization. J Cell Physiol 2010; 225: 701-708.
[15] Grimsholm O, Rantapaa-Dahlqvist S and Forsgren S. Levels of gastrin-releasing peptide and substance P in synovial fluid and serum correlate with levels of cytokines in rheumatoid arthritis. Arthritis Res Ther 2005; 7: R416-426.
[16] Lee JB, Park HN, Ko WK, Bae MS, Heo DN, Yang DH and Kwon IK. Poly (L-lactic acid)/hydroxyapatite nanocylinders as nanofibrous structure for bone tissue engineering scaffolds. J Biomed Nanotechnol 2013; 9: 424-429.
[17] Ezirganli S, Polat S, Baris E, Tatar I and Celik HH. Comparative investigation of the effects of different materials used with a titanium barrier on new bone formation. Clin Oral Implants Res 2013; 24: 312-319.
[18] Guillaume O, Naqvi SM, Lennon K and Buckley CT. Enhancing cell migration in shape-memory alginate-collagen composite scaffolds: in vitro and ex vivo assessment for intervertebral disc repair. J Biomater Appl 2015; 29: 1230-1246.
[19] Liu T, Huang Y, Guo L, Cheng W and Zou G. CD44+/CD105+ human amniotic fluid mesenchymal stem cells survive and proliferate in the ovary long-term in a mouse model of chemotherapy-induced premature ovarian failure. Int J Med Sci 2012; 9: 592-602.
[20] Walmsley GG, McArdle A, Tevlin R, Momeni A, Atashroo D, Hu MS, Feroze AH, Wong VW, Lorenz PH, Longaker MT and Wan DC. Nanotechnology in bone tissue engineering. Nanomedicine 2015; 11: 1253-1263.
[21] Denry I and Kuhn LT. Design and characterization of calcium phosphate ceramic scaffolds for bone tissue engineering. Dent Mater 2016; 32: 43-53.
[22] Wu W, Zhou Y and Tan W. [In vitro culture of bone marrow-derived mesenchymal stem cells in a chemically-defined serum-free medium]. Sheng Wu Gong Cheng Xue Bao 2009; 25: 121-128.
[23] Korkusuz P, Kose S and Kopru CZ. Biomaterial and stem cell interactions: histological biocompatibility. Curr Stem Cell Res Ther 2016; 11: 475-486.